COMPUTATIONAL CONTINUUM MECHANICS

ВЫЧИСЛИТЕЛЬНАЯ МЕХАНИКА СЛОШНЫХ СРЕД

Computational Continuum Mechanics. 2022. Vol. 15. No. 1. pp. 56-66 DOI: 10.7242/1999-6691/2022.15.1.5

INVESTIGATION OF COMPUTATIONAL MESHES FOR MODELING THE AIR DYNAMICS IN A VORTEX TUBE CHANNEL BY OPENFOAM SOFTWARE

C.I. Mikhaylenko

Mavlyutov Institute of Mechanics UFRC RAS, Ufa, Russian Federation

A vortex tube is a simple device without moving parts that separates a swirling gas stream into two vortexes, different in temperature, usually above or below the temperature of the inlet gas. This paper presents the mathematical model of a vortex tube which is based on gas dynamics laws and supplemented by a $k-\omega$ turbulence model. A description of the technique is given for constructing a finite-volume mesh with definition of the near-wall region based on the blockMesh utility when the conditions for the uniformity of the mesh elements are met while maintaining their orthogonality. The numerical solution is carried out on a computational cluster using the sonicFoam solver of the OpenFOAM free software. Three episodes of numerical simulation experiments were carried out to determine the temperature distribution in the channel of a cold air diaphragm depending on the diaphragm diameter. Each episode uses a grid of one of the three scales specified in the study: rough, normal, or fine. It is shown that mesh size reduction improves the convergence of simulation results. It is also demonstrated that qualitatively correct results can be obtained by generating a mesh in which the average linear size of a finite volume does not exceed 0.4 mm (0.025 in dimensionless representation). To improve the accuracy of quantitative data, an even greater computational mesh size reduction is required; in particular, a fine mesh with an average linear size of the finite volume less than 0.02 is considered in this work. The results obtained on a fine mesh are in good agreement qualitatively with the data for a tough mesh, but quantitatively the numerical values can differ significantly. This is shown in the calculations for a large diameter of the cold air diaphragm. Thus, when modeling a computational mesh for a vortex tube, it is necessary to maintain a balance between the required modeling accuracy and the time spent on its implementation.

Key words: finite-volume mesh, numerical simulation, OpenFOAM, vortex tube, turbulence

1. Introduction

The vortex tube effect, also referred to as the Ranqie–Hilsch effect, is a phenomenon associated with the separation of a compressed air stream into two vortexes with temperatures above and below the initial temperature of the injected air. The effect is produced in a simple mechanism such as cyclone, characterized by complete absence of moving parts.

The vortex tube effect and a device, which makes the effect and subsequently called the vortex tube, were discovered by Georges Joseph Ranque in 1931, as he reported at the conference in 1933 [1]. However, his results caused a skeptical reaction, so the second publication describing the effect turned out to be a much later written article by Rudolf Hilsch [2], published in 1947 in a regular journal and managed to arouse interest to the discussed phenomena. This interest is well confirmed by the fact that a review of articles about vortex tubes and the Ranque–Hilsch effect [3], published in 1954, contained more than a hundred references.

There are a lot of applications of vortex tubes because of its simple design. So, in addition to trivial use in refrigeration equipment and for cooling plants and chemical reagents, the Ranque–Hilsch tubes can provide control and stabilization of the temperature for diving, hyperbaric chambers, NMR equipments, gas drying, phase separation, including disperse phase separation, as well as temperature stabilization in a nuclear reactors [4–8].

Of particular interest are publications showing this effect not only for gases but also for liquids [9, 10].

It is important to note that research of the vortex tube effect continues these days. The constant increase in the number of publications number devoted to vortex tubes [11–13], is due to the lack of an unambiguously working explanation of the nature of the Ranque-Hilsch effect formation. Thus, Piralishvili's monograph [14] outlines the main theories for the vortex effect, however, all of them

Email addresses for correspondence: const@uimech.org

have a common drawback, which is that each of the theories has predictive power only within the parameters of some particular cases. So, to construct new devices with vortex effect and modify existing ones, as well as in order to search for a full-fledged theory to explain the mechanism of the effect, a significant amount of research is being carried out. As shown in the reviews [11–13] mentioned above, in the absence of a valid theory, the main approaches to the study and development of vortex tubes are still physical and numerical experiments. Both directions have their own advantages and disadvantages.

When conducting numerical simulation, if we exclude the stage of selection and justification of the applied mathematical model, but take into account the proposed numerical method, the main difficulty will be a mesh of nodal points. In the work, we used the mesh of finite volumes, which satisfies some parameters, such as uniformity, weak distortion, orthogonality. The development of a finite volume mesh with the same parameters was described in the articles [15, 16]. In [15], several variants for placing hexahedral blocks when constructing a mesh in the OpenFOAM software are considered, where a hexahedral mesh is made for a geometrically full model of a vortex tube. In [16], a version of the mesh with a periodical boundary conditions were successfully applied only for a quarter of the vortex tube volume. It was shown that this approach does not affect simulation results, however, it can significantly reduce the simulation time.

In this paper, we evaluate the influence of a mesh size on the data of numerical simulation describing the Ranque–Hilsch effect. The model of a vortex tube, is being studied, for which, due to the use of periodic boundaries with rotational symmetry with a period $\pi/2$, a quarter of the described volume is covered. The qualitative and quantitative analysis is done of the physical values of the air in the cold outlet on meshes of different sizes using the example of changing the diameter of the cold side diaphragm.

2. Definition of the problem

2.1. Mathematical model

A swirling gas flow in a vortex tube channel can be described in terms of standard gas dynamics equations using an appropriate turbulence model [17, 18]. The need to use the turbulence model is dictated by the physical features of the vortex tube, as well as by the significant expenditure of computational resources, calculation time and hardware parameters if we use a direct numerical simulation of the processes under study [19].

Thus, in the problem under consideration, the air velocity can achieve over 400 m/s for a vortex tube with its channel diameter of 16 mm. Therefore, the lower estimated value for the Reynolds number will be $\mathrm{Re} = 10^5$ which indicates the obviously turbulent nature of the processes.

The mathematical model in the article includes

– continuity equation

$$\frac{\partial \rho}{\partial t} + \frac{\partial \left(\rho u_i \right)}{\partial x_i} = 0;$$

– momentum equation (the Navier–Stokes equation) in a vector form

$$\frac{\partial \left(\rho u_i \right)}{\partial t} + \frac{\partial \left(\rho u_i u_j \right)}{\partial x_j} = -\frac{\partial \rho}{\partial x_i} + \frac{\partial \tau_{ij}}{\partial x_j};$$

– equation of specific total energy

$$\frac{\partial(\rho E)}{\partial t}+\frac{\partial\left(\rho u_j E\right)}{\partial x_j}=-\frac{\partial\left(p u_j\right)}{\partial x_j}+\frac{\partial\left(\tau_{ik} u_k\right)}{\partial x_j};$$

– perfect gas equation of state

$$e=\frac{p}{(\gamma-1)\rho}.$$

Another relationships can be used as an equation of state, however, the simplest equation is enough for the investigation goals.

Calculation of temperature is based on a specific total energy value

$$T=\frac{1}{c_p}\left(E-\frac{1}{2}\boldsymbol{U}\boldsymbol{U}\right).$$

Here we use the notations: γ is an adiabatic coefficient; u_i are components of a velocity vector $\boldsymbol{U}$; i, j, k are coordinate indexes here and below; ρ is a gas density; $E=e+\left(\sum u_i^2\right)/2$ is a specific total energy of gas, which is written by specific internal energy e; p is pressure; $c_p=\gamma c_v$ is specific heat at constant volume; $c_v=1005$ J/K is specific heat at constant pressure, that is given in the model. The equation also has a stress tensor τ_{ij}:

$$\tau_{ij}=\left(\mu+\mu_t\right)\left[\left(\frac{\partial u_i}{\partial x_j}+\frac{\partial u_j}{\partial x_i}\right)-\frac{2}{3}\delta_{ij}\frac{\partial u_k}{\partial x_k}\right].$$

Here μ is a coefficient of dynamic viscosity; μ_t is a coefficient of turbulent dynamic viscosity, that is calculated by the formula $\mu_t=\nu_t\rho$, and ν_t is a coefficient of turbulent kinematic viscosity taken from the model of turbulence; δ_{ij} is Kronecker symbol.

The turbulence model $k-\omega$ chosen for this problem is characterized by high nonlinearity. However, it is convenient to apply the $k-\omega$ model with near-wall functions, that is, this model is well suited for calculating turbulence in regions with closely spaced walls, which is naturally represented by a vortex tube.

The $k-\omega$ model of turbulence belongs to the class of two-parameter models and can be described by two equations:

– equation for turbulent kinetic energy k

$$\frac{\partial k}{\partial t}+\frac{\partial\left(u_j k\right)}{\partial x_j}=\tau_{ij}\frac{\partial u_i}{\partial x_j}-\beta^*\omega k+\frac{\partial}{\partial x_j}\left[\left(\nu+\sigma^*\nu_t\right)\frac{\partial k}{\partial x_j}\right];$$

– equation for specific rate ω of turbulent energy dissipation

$$\frac{\partial\omega}{\partial t}+\frac{\partial\left(u_j\omega\right)}{\partial x_j}=\frac{\alpha\omega}{k}\tau_{ij}\frac{\partial u_i}{\partial x_j}-\beta\omega^2+\frac{\partial}{\partial x_j}\left[\left(\nu+\sigma\nu_t\right)\frac{\partial\omega}{\partial x_j}\right].$$

k and ω calculated by these equations, give a kinematic turbulent viscosity value $\nu_t=k/\omega$.

The above turbulence model equations include a number of empirical parameters with the following values

$$\alpha = 13/25, \quad \beta = 9/125, \quad \beta^* = 9/100, \quad \sigma = \sigma^* = 1/2.$$

2.2. Geometry of the modeling area

Simulation of a countercurrent vortex tube with a vortex chamber is carried out. The vortex chamber has an enhanced diameter and four inlet channels placed symmetrically along the axis of the tube. The hot outlet diaphragm is a narrow circular gap between tube walls and a truncated cone. Since the device has axial symmetry, the calculation time can be saved by reducing of the simulation area. In Figure 1 the scheme is shown of the simulation area of a vortex tube model used in this paper.

So, due to the rotational symmetry about the tube channel axis, in the presented case, by analogy with [16], only the fourth (i.e. assume a rotational period $\pi/2$) part of tube *1* with the main channel diameter equal D.was chosen for calculations. For the same reason, periodic boundary conditions are set at boundaries *2* . Another reason for choosing a computational area with periodic boundaries is related to the simulation time. The introduction of periodic conditions at the boundaries makes it possible to obtain an almost fourfold gain in time during simulation.

Figure 1 also shows area *3* with an inlet channel, which bring pressed gas to the vortex chamber *4*. We assume that diameter of the vortex chamber is equal $1{,}1D$. The dimensions of the vortex chamber are determined by the diameter of the inlet channel. Structural design of the vortex chambers can be very diverse, but its main goal is to ensure the swirling flow formation of tangentially or close to the tangential direction of the injected gas.

The channel of the cold outlet diaphragm *5* begins from the end of the vortex chamber wall placed in the center, designed to remove cold air. A cone of a throttle makes a hot air side of diaphragm *6*. This diaphragm is for hot air outlet, produced at the near-wall area of air flow. The central frustum of the cone mirrors a downflow vortex.

Finally, the areas for gas outlets, which have special boundary conditions, have number *7*. These areas are removed from the actual hot and cold outlets of a vortex tube to reduce the influence of the boundary conditions on the dynamics of the outlet gas. Discussion about boundary conditions and their influence on the results of a vortex tube simulation are given in the article [20].

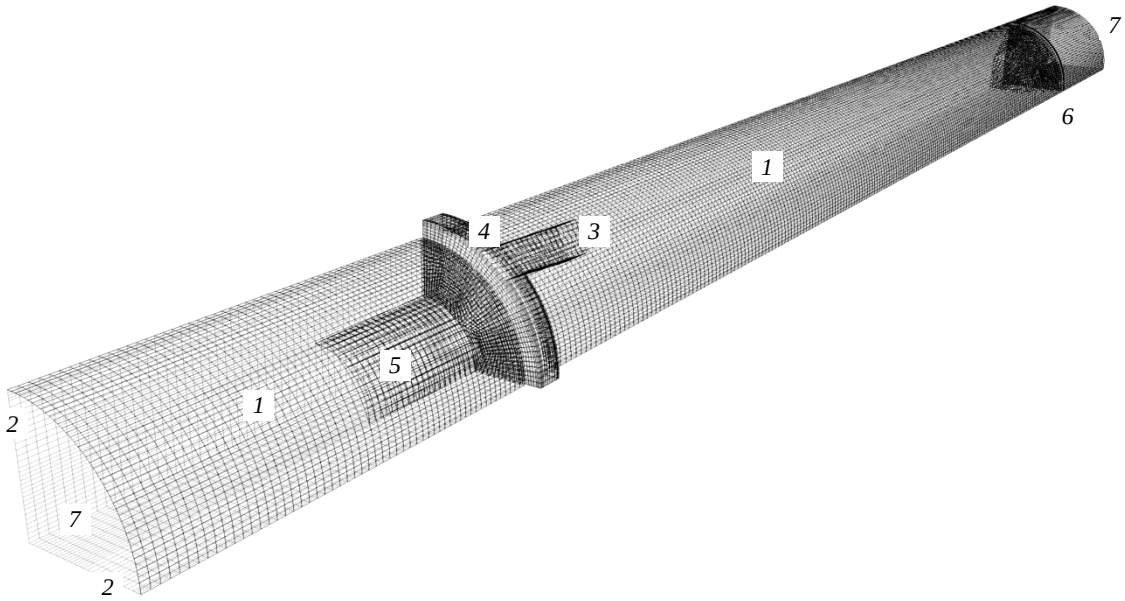

Figure 1. The simulation area scheme: walls (*1*) are drawn with a dark grid; periodical boundaries (*2*) are marked with lighter grid; the pressed gas injection area with inlet tube (*3*); vortex chamber (*4*); the cylindrical outlet channel of the cold air diaphragm (*5*); frustum of the cone of the hot outlet diaphragm (*6*); and the areas with boundary conditions for outlet gas (*7*).

In the present work, we used a counter flow vortex tube scheme, which has the following parameters. The main channel length is $L = 120$ mm and its diameter is $D = 16$ mm; the pressed air injection is organized with four inlet tubes, which have square section and their sizes are 2×2 mm, also these tubes have an angle of 40 degrees with the tangential direction; the vortex chamber diameter is $1{,}1D$; the hot side diaphragm is frustum of a cone, which has the top diameter of 8 mm and the ground diameter, which is calculated from the hot diaphragm gap size ($h = 4$ mm); the cold diaphragm diameter was taken from 5 to 12 mm. In other words, a series of problem is considered for the values of the dimensionless parameter $d/D = 0{,}3 \div 0{,}75$. The cold side diaphragm is opened to a cylindrical channel of length $l = 10$ mm and its diameter equals to the diameter of the diaphragm. Gas outlets of cold and hot diaphragms have a distance to faces with outlet boundary conditions. This distance equals to 20 mm.

2.3. Initial and boundary conditions

At the initial moment of time $t = 0$, it is considered that the gas (air) is under normal thermodynamics conditions and is stationary, i.e. over the entire simulated area, speed is $\boldsymbol{U}^0 = 0$ m·s^{-1}, temperature is $T^0 = 293$ K, and pressure equals to barometric $p^0 = 100$ kPa, initial density is calculated from the equation of state. The turbulence parameters (turbulence kinetic energy and its specific dissipation rate) are taken constant over the entire area and their values are $k = 5$ m^2·s^{-2} and $\omega = 0{,}5$ s^{-1}.

On the inlet it is accepted that the injected air has the same temperature as the initial $T_{\text{inlet}} = T^0 = 293$ K; the pressure is $p_{\text{inlet}} = 650$ kPa, that is often used value in experiments; velocity (i.e. volumetric or mass rate of air flow) is dictated by the pressure gradient; turbulent kinetic energy and specific rate of turbulent kinetic energy dissipation are constant and equal to initial values.

In the outlets, pressure is assumed close to atmospheric ($p_{\text{outlet}} = 100$ kPa) and all other physical parameters have flow boundary conditions, i.e. the normal derivative equals zero, the no-slip boundary conditions are assigned on solid walls and near-walls functions for the turbulence are specified. In OpenFOAM software, the function kqRWallFunction is used, which models Neumann boundary conditions for the turbulent kinetic energy k. The specific rate of turbulent energy dissipation is described by boundary function omegaWallFunction with constant value $\omega = 0{,}01$ s^{-1}.

3. Finite volume mesh structure

3.1. Finite volume mesh creating and development

The finite volume mesh is made by blockMesh utility, which is a part of OpenFAOM software. There are steps of data preparing for the mesh generating. First, spatial coordinates of hexahedrons' vertexes are described, then vertexes are connected with each other and organize hexahedrons' faces. These resulting hexahedral blocks are divided into smaller finite volumes, taking into account the fact that the number of finite volumes and their vertexes on common faces of the two adjacent blocks should be the same.

The construction of a finite-volume mesh for a vortex tube is associated with a number of complexities, which are effects of a simulation area structure. There is a system of nested coaxial cylinders, which has an axis common with the axis of a vortex tube main channel (see Figure 2). Figure 2 shows the cross sections for two constructions of a vortex tube with the following division into blocks of hexahedrons (described from the center to the periphery): the central block *1* with the radius, that assigned with the cold air diaphragm radius. Block *2* is between internal area by the block *1* and near-wall layer (block *3*). The radius of block *3* equals the main channel radius of a vortex tube. A vortex chamber is described with block *4*.

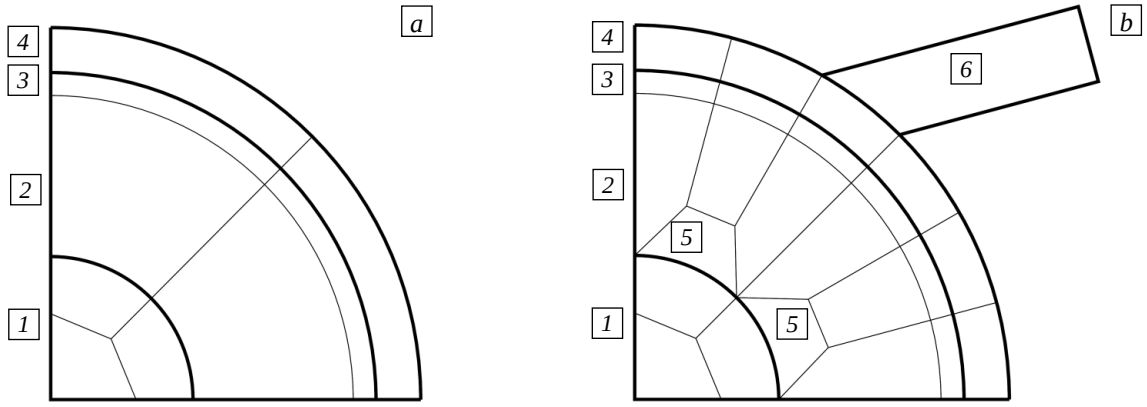

Figure 2. The scheme of hexahedral blocks (*1–4*) positioning on the cross section of the simulated area: the standard area splitting for the nested cylinders case (*a*); the splitting is used in the presented article (*b*), which includes additional blocks *5* and inlet channel block *6*.

This nesting of cylinders makes it difficult to mesh a cylindrical area. It is known that the best quality mesh for a cylinder consists of five blocks, the central hexahedron and four surrounding it. As the simulated area is a sector with the angle $\pi/2$ of an initial tube model, in its representation, due to symmetry, it is enough to consider three blocks out of five. After splitting these blocks into finite volumes, the resulting mesh is characterized by good uniformity and is sufficiently orthogonalized. However, in a situation where the innermost cylinder has a relatively small radius, and the mesh constructing method, that is described above, is unchanged throughout the computational area, the mesh loses uniformity in cylinders with a larger radius, since their finite volumes is tangentially longer and radially shorter vs ones into the inner cylinder, where finite volumes have the same volumetric size (see the figure 2*a*, blocks *2–4*).

Thus, it is necessary to take some special actions, when dividing the computational area considered in this paper into elements in order to preserve the uniformity of finite volumes and, at the same time, not to violate their orthogonality.

Figure 2*b* shows the scheme of the simulated area splitting in cross section for the developed variant of hexahedron configuration. In order to increase the number of finite volumes in the tangential direction, additional blocks are introduced, indicated by the number *5*. It can be seen in the scheme that this approach leads to triplication of finite volume quantity in the external cylinders, and their tangential size becomes comparable to the finite volume sizes into the central area.

However, the introduction of additional blocks leads to distortion of the shape (non-orthogonality) of finite volumes adjacent to the boundaries of these blocks. As a result, some finite volumes can have angle between a pair of edges much different form right one. But, despite the obvious deviation from orthogonality, critical values are not reached, and the finite-volume mesh built according to this approach fully complies with the requirements of OpenFOAM and passes the test conducted by the checkMesh utility without any errors or warnings.

In the direction along the tube axis, several zones are also distinguished (see Figure 1): “cold” boundary, the channel of the cold outlet diaphragm; the vortex chamber with additional blocks *4* and *6* shown in Figure 2*b*; the main channel of a vortex tube with the cone of the hot outlet diaphragm; the “hot” boundary. Thus, the computational mesh for the vortex tube studied in this work is constructed by the blockMesh utility with uniform splitting of 92 hexahedrons into finite volumes.

3.2. Modeling mesh sizes

Three episodes of numerical simulation were carried out in the investigation. The gas dynamics in a vortex tube was simulated for different diameters of the cold side diaphragm. For each episode eight calculations were performed with sequential changing in the diameter of the cold diaphragm from 5

to 12 mm in increment of 1 mm. All episodes differed from each other both in the size of finite volumes of their grids and their numbers, the corresponding parameters are presented in Table 1.

The average number of finite volumes in the roughest mesh can be estimated at 86000. The average calculation time in one model problem for a time period from zero to 0.1 s on twelve processor cores takes approximately 40 hours. For a mesh of conventionally standard size with an average number of finite volumes of about 175000, the calculation time is about 90 hours. Finally, with the finest of the meshes tested (with approximately 265000 finite volumes), the simulation time reaches 145 hours.

Thus, with an increase in the number of finite volumes, the calculation time increases linearly. The fact can be fully explained, since the approach used in spatial decomposition, such as decomposition style, numerical algorithm and spatial area are in good agreement with the conditions necessary for a completely parallel solution of the problem [21].

Table 1. Parameters of meshes and duration of numerical simulations

The episode number	The caliber of the mesh	The average number of finite volumes	The average finite volume linear size ℓ, mm	The average simulation tine, s
1	rough	86039	0,462	148405
2	standard	174870	0,365	329951
3	fine	267547	0,317	522856

In Table 1, the average values of linear sizes of finite volumes for all kinds of meshes are also shown. It is clear that finite volume number doubling leads to the decrease of linear sizes of each volume on $\sqrt[3]{2}$ times. However, even such a change in volume size (as it will be shown below) affects the quantitative results.

4. Results and discussion

4.1. Hardware and software

The numerical simulations were performed on the supercomputer at Ufa State Aviation Technical University [22]. Each numerical experiment was run on a separate node and executed 12 cores, to eliminate data transfer losses. Linear spatial decomposition of the modeling area was carried out only by one coordinate, along the symmetry axis of the vortex tube channel.

We used OpenFOAM free software [23] for our simulations. The finite volume mesh for a studied tube was generated by the blockMesh utility. The standard solver sonicFoam turned out to be sufficient for calculation the problems with small changes that determined physical and mechanical parameters of the injected medium.

The described approach makes it possible to get results that fully correspond to the problem solution and allow us to draw conclusions about the dynamics of the processes both in the vortex tube channel and at the outlets [24].

4.2. Relaxation of the process in numerical simulations

The problem under consideration is essentially non-stationary, however, after a certain time period, all calculated physical parameters come to quasi-periodical pulsations about the average values. In this regard, it is possible to talk only about the establishment of a solution only based on the evaluation of time-averaged results, when changes in one or another calculated physical parameter deviate from a certain value by a small relative amount.

Thus, during the calculations, the time value was empirically obtained, which can be considered the moment of establishing the simulated process in the sense of quasi-periodic pulsations of the

average values of the investigated physical parameters. The relaxation is observed at the time about 0.05–0.06 s from the beginning of simulation.

In connection with the found time of relaxation, a range of values of 0.07–0.1 s was used for time averaging of all considered physical parameters.

4.3. Distribution of the temperature along the cold outlet channel

Let us estimate the simulation results for three different meshes, used for the investigation of cold air production dependence from the only geometrical parameter, that is a diameter of a cold side diaphragm. The dependences of the air temperature along a cold air outlet channel on the diaphragm diameter are shown in Figure 3. The data of three episodes of computational experiments described in section 3.2, are shown: the results for "rough" mesh are shown in Figure 3*a*, the "normal" mesh results are shown in Figure 3*b* and the "fine" mesh ones are shown in Figure 3*c*. In all Figures, the reduced length of the cold outlet channel is set horizontally, and the ratio of the cold diaphragm to the diameter of the main channel of the vortex tube is set vertically. The color levels indicate the air temperature normalized by the injected gas temperature T_0.

The temperature in every point was calculated by the double averaging. First, we calculated the average value for the cross-section along the channel, and then these results were averaged over several time steps in order to avoid the quasi-periodic pulsation affect.

Figure 3 shows the weak qualitative dependence of the results on a mesh scale, but quantitatively they can differ markedly. Thus, we can see in Figure 3*c* that the gas temperature on the cold side outlet channel with the fine mesh for big ratios d/D exceeds not only the temperature obtained with other mesh scales, but also the temperature of the injected gas T_0.

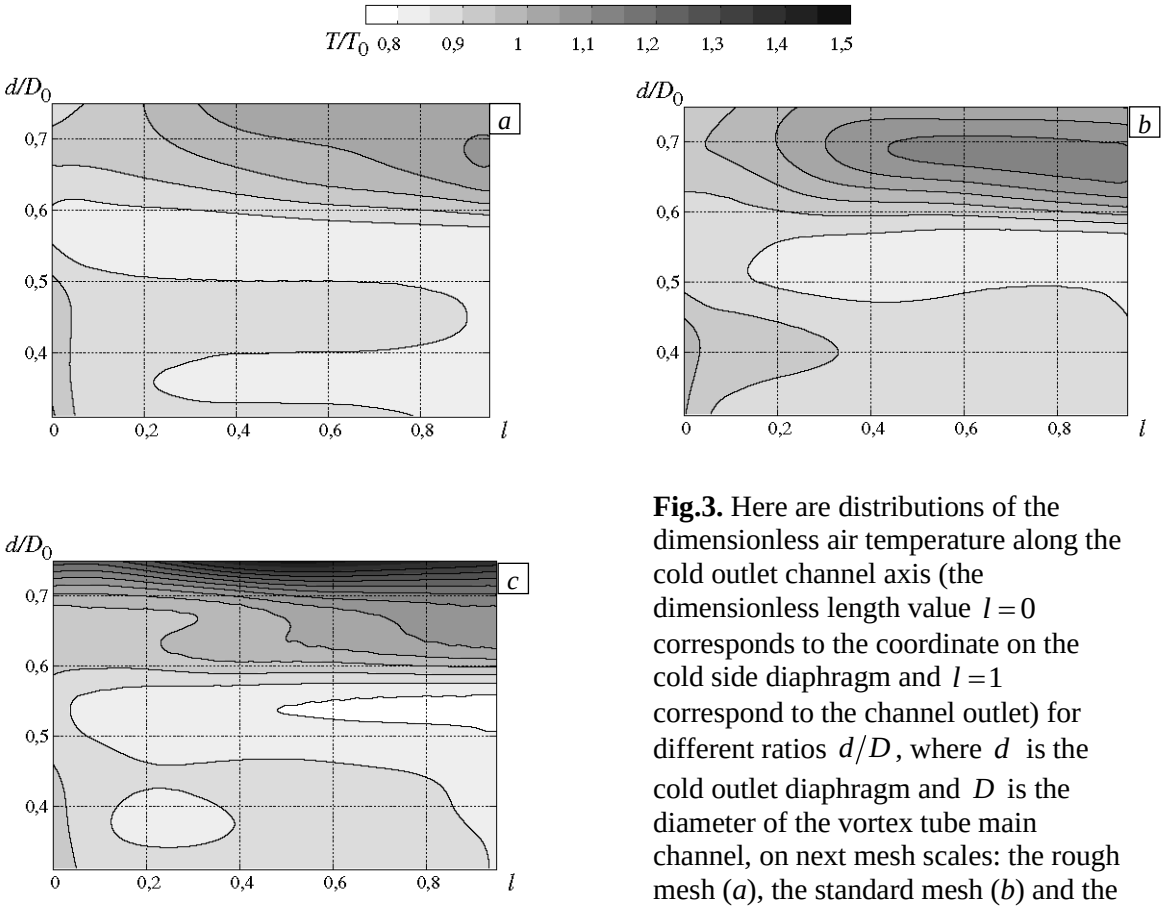

Fig.3. Here are distributions of the dimensionless air temperature along the cold outlet channel axis (the dimensionless length value $l=0$ corresponds to the coordinate on the cold side diaphragm and $l=1$ correspond to the channel outlet) for different ratios d/D, where d is the cold outlet diaphragm and D is the diameter of the vortex tube main channel, on next mesh scales: the rough mesh (*a*), the standard mesh (*b*) and the fine one (*c*).

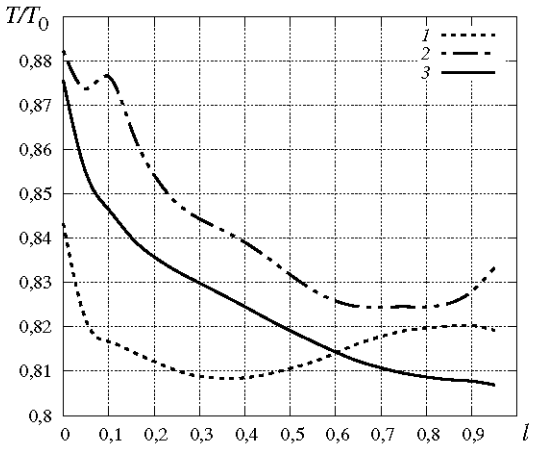

Figure 4. The distributions of the dimensionless temperature along the cold side outlet channel with the relation $d/D = 0,56$ for different meshes: the rough mesh with number of finite volumes equals 93325 (the curve *1*), the standard mesh (164520 finite volumes, the curve *2*) and the fine one (264810 finite volumes, the curve *3*).

Let us consider the results of simulations in terms of finding the minimal temperature value at the cold outlet. For this case in Figure 3 we can see that temperature minimum is independent from a mesh scale, the minimum is at the relation value $d/D = 0,56$, or in other words, if the cold diaphragm diameter is $d = 9$ mm.

In Figure 4 the curves of the dimensionless temperature values, which was averaged on cross section and time, along the cold outlet channel are shown for the three discussed finite volume meshes, for the model case $d = 9$ mm. Qualitatively, the temperature distribution obviously differs only on the roughest mesh (curve *1*). In this case, the area of the minimum temperature of the outlet gas is shifted to the cold diaphragm (to the dimensionless coordinate $l = 0$). When the number of finite volumes increases (refining the mesh to standard (*2*) and fine (*3*) scales), the difference is rather quantitative. The result on a more detailed mesh only indicates that the temperature of the outlet air is lower.

Table 2 contains calculation parameters for three calibers of meshes. These simulations were performed for the vortex tube with the cold side diaphragm diameter $d = 9$ mm. In consideration of the above discussion of the curves in Figure 4 and the data from the Table, it can be concluded that the choice should be between the standard mesh, which has the average finite volume linear size $\ell < 0,4$ mm (or dimensionless size $\tilde{\ell} < 0,025$, where $\tilde{\ell} = \ell/D$) and the fine mesh, where the average linear size is $\ell \le 0,3$ mm ($\tilde{\ell} < 0,02$). With this choice, the balance will be maintained between the counting time and good quality (accuracy) of the results.

Table 2. Parameters of finite volume meshes and their simulation time for the geometry with relation $d/D = 0,56$

The episode number	The caliber of the mesh	The number of finite volumes	The average finite volume linear size ℓ, mm	The dimensionless average finite volume linear size $\tilde{\ell} = \ell/D$	The simulation tine, s
1	rough	93325	0.449	$2.9 \cdot 10^{-2}$	161717
2	standard	164520	0.372	$2.3 \cdot 10^{-2}$	291712
3	fine	264810	0.317	$2.0 \cdot 10^{-2}$	510518

5. Conclusions

In the article, it was found that the finite volume meshes constructed in accordance with the method described in section 3, while maintaining uniformity and orthogonality, leads to the qualitatively similar results with an average linear size of the finite volume less than 0.4 mm. Thus, in order to estimate the behavior of the gas in the vortex tube channel we can use relatively rough meshes to reduce the duration of computational experiment and calculation time. In this work, the term “not very fine” can be applied to the mesh denoted as “standard”.

It should be noted that the approach of mesh making is efficient when implemented on multiprocessor computing devices, with the fulfillment of some simple requirements it is possible to achieve almost linear acceleration of calculations. Important for further research is the fact that the discrete analog of the simulation area, i.e., a mesh constructed according to the scheme of Section 3, makes it possible to perform calculations in a significant range of values of a number of geometrical parameters of the vortex tube.

It was also found that mesh refinement changes the quantitative results. This fact can indicate the convergence of the numerical simulations. For greater reliability, it is necessary to compare the results of the experiments and numerical simulations on different mesh scales. The implementation of such a comparison is planned by the author in future.

The availability of qualitatively correct simulation data of the vortex tube makes it possible to use the computational meshes described in this work in numerical simulations aimed at in-depth studies and explanation of the physical mechanism of the vortex effect.

The numerical simulations were carried out on the computer cluster of USATU, Ufa [22]. The study was supported by the state budget (state task 246-2019-00520 for 2019-2022).

References

1. Ranque G.J. Experiments on expansion a vortex with simultaneous exhaust of hot air and cold air. *Journal de Physique et Le Radium*, 1933, vol. 4, pp. 112-114.
2. Hilsch R. The use of the expansion of gases in a centrifugal field as cooling process. *RSI*, 1947, vol. 18, pp. 108-113. https://doi.org/10.1063/1.1740893
3. Westley R. *A bibliography and survey of the vortex tube*. College of Aeronautics, Cranfield, UK, 1954. 38 p.
4. Bruno T.J. Laboratory applications of the vortex tube. *J. Chem. Educ.*, 1987, vol. 64, pp. 987-988. https://doi.org/10.1021/ed064p987
5. Baz A., Gilheany J., Kalvitas A. Feasibility of vortex tube assisted environmental control of an underwater research habitat. *Ocean Eng.*, 1988, vol. 15, pp. 33-54. https://doi.org/10.1016/0029-8018(88)90018-2
6. Zhang B., Guo X. Prospective applications of Ranque–Hilsch vortex tubes to sustainable energy utilization and energy efficiency improvement with energy and mass separation. *Renew. Sustain. Energ. Rev.*, 2018, vol. 89, pp. 135-150. https://doi.org/10.1016/j.rser.2018.02.026
7. Martin R.W., Zilm K.W. Variable temperature system using vortex tube cooling and fiber optic temperature measurement for low temperature magic angle spinning NMR. *J. Magn. Reson.*, 2004, vol. 168, pp. 202-209. https://doi.org/10.1016/j.jmr.2004.03.002
8. Kumar A., Vivekanand, Subudhi S. Cooling and dehumidification using vortex tube. *Appl. Therm. Eng.*, 2017, vol. 122, pp. 181-193. https://doi.org/10.1016/j.applthermaleng.2017.05.015
9. Balmer R.T. Pressure-driven Ranque-Hilsch temperature separation in liquids. *J. Fluid. Eng.*, 1988, vol. 110, pp. 161-164. https://doi.org/10.1115/1.3243529
10. Akhmetov D.G., Akhmetov T.D. Flow structure and mechanism of heat transfer in a Ranque–Hilsch vortex tube. *Exp. Therm. Fluid. Sci.*, 2020, vol. 113, 110024. https://doi.org/10.1016/j.expthermflusci.2019.110024
11. Eiamsa-ard S., Promvonge P. Review of Ranque–Hilsch effects in vortex tubes. *Renew. Sustain. Energ. Rev.*, 2008, vol. 12, pp. 1822-1842. https://doi.org/10.1016/j.rser.2007.03.006
12. Subudhi S., Sen M. Review of Ranque–Hilsch vortex tube experiments using air. *Renew. Sustain. Energ. Rev.*, 2015, vol. 52, pp. 172-178. https://doi.org/10.1016/j.rser.2015.07.103
13. Guo X., Zhang B., Liu B., Xu X. A critical review on the flow structure studies of Ranque–Hilsch vortex tubes. *International Journal of Refrigeration*, 2019, vol. 104, pp. 51-64. https://doi.org/10.1016/j.ijrefrig.2019.04.030
14. Piralishvili Sh.A. *Vikhrevoy effekt. T. 1. Fizicheskoye yavleniye, eksperiment, teoreticheskoye modelirovaniye* [Vortex effect. Vol. 1. Physical phenomenon, experiment, theoretical modeling]. Moscow, Nauchtekhlitizdat, 2013. 343 p.
15. *Mikhaylenko C.I.* Simulation of the vortex tube: design of a hexagonal mesh for computational experiments in OpenFOAM. *Trudy Instituta mekhaniki im. R.R. Mavlyutova UNTs RAN – Proceedings of the Mavlyutov Institute of Mechanics*, 2016, vol. 11, no. 1, pp. 112-118. https://doi.org/10.21662/uim2016.1.017

16. Mikhaylenko C.I. Building a finite-difference mesh and selecting a turbulence model for numerical simulations of a vortex tube in OpenFOAM software. *J. Phys.: Conf. Ser.*, 2020, vol. 1677, 012021. https://doi.org/10.1088/1742-6596/1677/1/012021
17. Bianco V., Khait A., Noskov A., Alekhin V. A comparison of the application of RSM and LES turbulence models in the numerical simulation of thermal and flow patterns in a double-circuit Ranque-Hilsch vortex tube. *Appl. Therm. Eng.*, 2016, vol. 106, pp. 1244-1256. https://doi.org/10.1016/j.applthermaleng.2016.06.095
18. Dutta T., Sinhamahapatra K.P., Bandyopdhyay S.S. Comparison of different turbulence models in predicting the temperature separation in a Ranque–Hilsch vortex tube. *International Journal of Refrigeration*, 2010, vol. 33, pp. 783-792. https://doi.org/10.1016/j.ijrefrig.2009.12.014
19. Marin D.F., Mikhaylenko C.I., Khaziev L.H. *Parallel computing technologies (PaVT'2011), 28 March-1 April 2011, Moscow. South Ural State University, 2011. Pp. 539-547.*
20. Minibaev M.R., Mikhaylenko C.I. Investigation of the influence of boundary conditions in the numerical solution of a vortex tube model. *Mnogofaznyye sistemy – Multiphase Systems*, 2019, vol. 14, no. 2, pp. 89-100. https://doi.org/10.21662/mfs2019.2.013
21. Gazizov R.K., Lukashchuk S.Yu., Mikhaylenko K.I. Razrabotka parallel'nykh algoritmov resheniya zadach mekhaniki sploshnoy sredy na osnove printsipa prostranstvennoy dekompozitsi [Development of parallel algorithms based on the principle of spatial decomposition for solving problems of continuum mechanics]. *Vestnik UGATU – Vestnik USATU*, 2003, vol. 4, no. 1, pp. 100-107.
22. https://www.ugatu.su/supercomputer/ (accessed 1 March 2022)
23. The OpenFOAM Foundation. https://openfoam.org/ (accessed 1 March 2022)
24. Mikhaylenko C.I. Vortex tube modelling: outlet parameter dependencies of cold air production. *J. Phys.: Conf. Ser.*, 2019, vol. 1158, 032032. https://doi.org/10.1088/1742-6596/1158/3/032032

The authors declare no conflict of interests.
The paper was submitted 23.06.2021; approved after reviewing 21.01.2022; accepted for publication 28. 01.2022